



Atmospheric Sciences

PhD Prospectus

Christian Nairy

University of North Dakota – Department of Atmospheric Sciences

21 November 2025

Committee Members:

Dr. David Delene (Chair) – UND Department of Atmospheric Sciences

Dr. Andrew Detwiler – UND Department of Atmospheric Sciences

Dr. Hallie Chelmo – UND Department of Mechanical Engineering

Dr. John Yorks – NASA Goddard, Earth Sciences Division



- **Introduction (*Chapter 1*)**
 - Big Picture
 - Background
 - Motivation
 - Dissertation Objectives
 - Main Hypotheses

- **Paper 1 (*Chapter 2*): In situ Observations of Ice Crystal Chain Aggregates in Winter Storms**
 - Brief Overview
 - Data & Methods
 - Results
 - Discussion
 - Conclusion
 - Status

- **Paper 2 (Chapter 3): Machine Learning Classification of Ice Crystal Chain Aggregates in Aircraft-Collected Cloud Particle Imagery**
 - Objectives
 - Data & Methods
 - Preliminary Results
 - Research Contributions
 - Status
- **Paper 3 (Chapter 4): Ice Crystal Chain Aggregates in Cold-Season Storms: Campaign-Scale Mapping and Contextualization* or Investigating the Spatio-Temporal Distribution of Ice Crystal Chain Aggregates in Winter Storms: Findings from the NASA IMPACTS Campaign***
 - Objectives
 - Data & Methods
 - Research Questions
 - Preliminary Results
 - Research Contributions
- **Collaborations (Non-Dissertation)**
- **Timeline to Graduation**

Introduction – Big Picture

- Ice aggregates form through aerodynamic, inertial, and gravitational interactions (Finnegan & Pitter, 1988).
- Lab work shows elongated chain aggregates when strong electric fields are applied (Fig. 1).
- Recent in-situ observations show chain aggregates (Fig. 2) across diverse cloud regimes and regions, in both summer and winter storms.
- Gap in understanding: Strong E-Field lab result \neq broad winter occurrence in observations \rightarrow our current picture is incomplete.
- **We still don't know when/where they form in cloud systems or how to recognize them reliably at scale.**

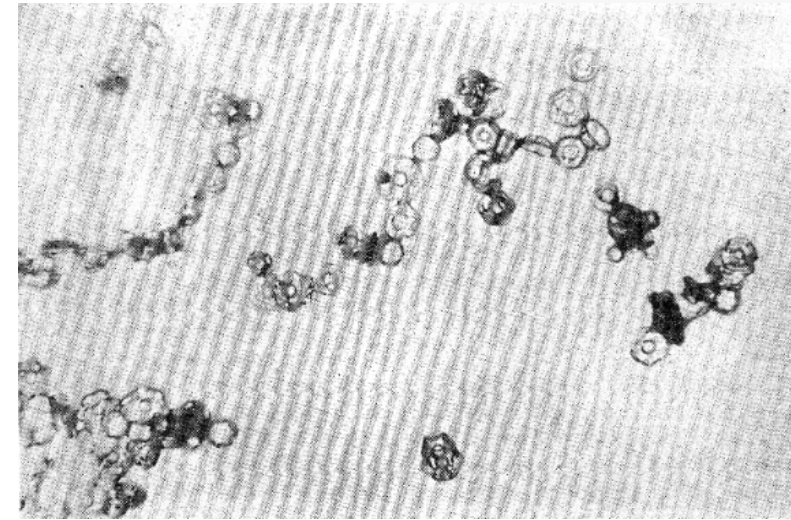


Fig. 1) Chains of ice crystals formed in the Manchester cloud chamber at $-12\text{ }^{\circ}\text{C}$ under a high (120 kV m^{-1}) electric field. Adapted from Saunders and Wahab, 1975.

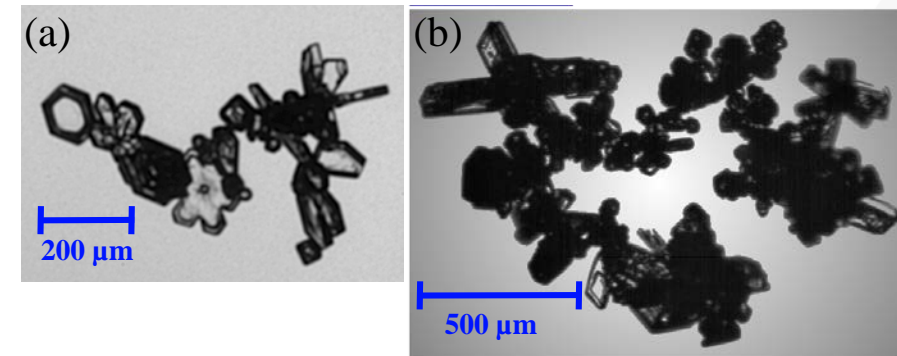
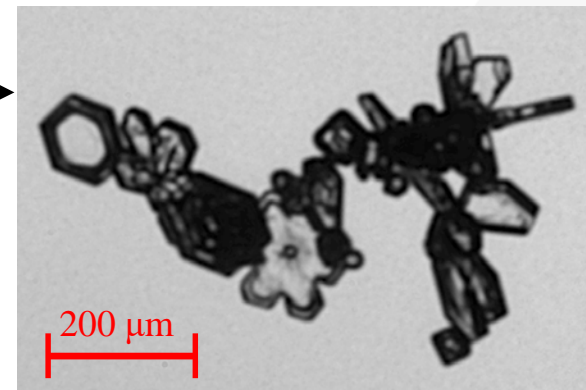
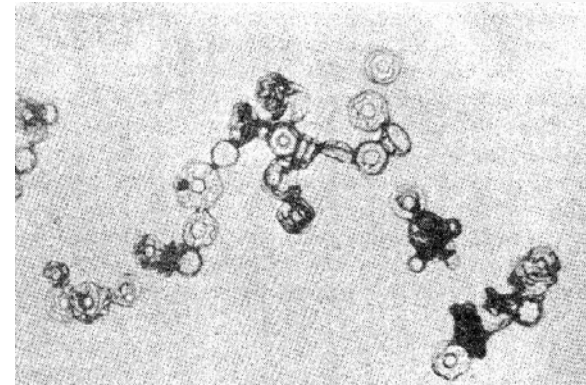


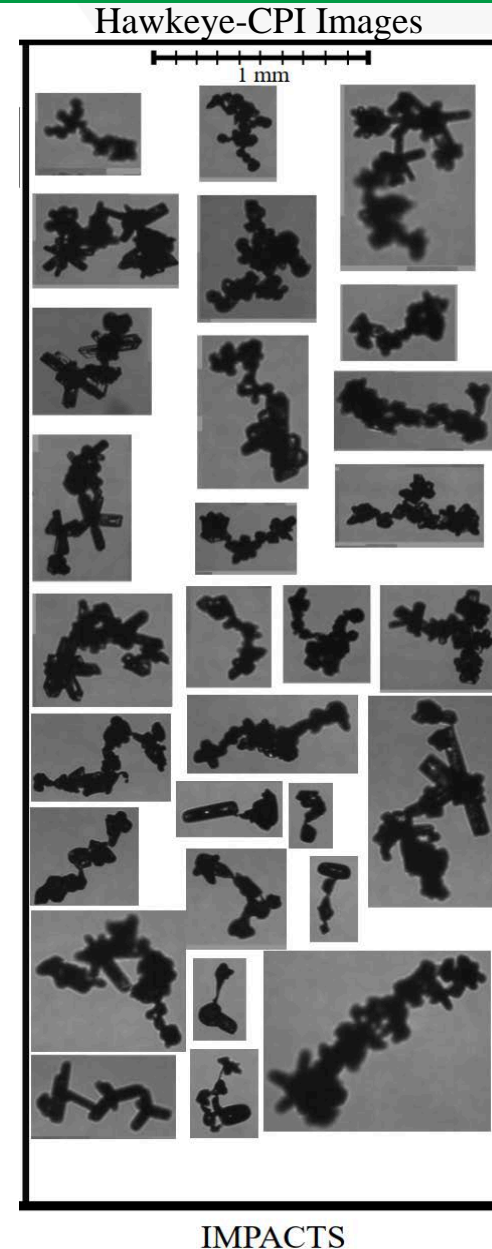
Fig. 2) Ice crystal chain aggregates observed in-situ during (a) the CapeEx19 Field Campaign on 3 August 2019 and (b) the Investigation of Microphysics and Precipitation for Atlantic Coast-Threatening Snowstorms (IMPACTS) on 15 February 2023.

Background (More Specifics)

- Chain Aggregate: Unusually elongated, quasi-linear ice crystal aggregate consisting of three or more discernable ice monomers joined together end-to-end or by small joints (Nairy, 2022).
- Laboratory experiments show that chain aggregation occurs in the presence of strong electric fields ($>60 \text{ kV m}^{-1}$) between -5 and $-37 \text{ }^{\circ}\text{C}$ (Maximum efficiency at $-8 \text{ }^{\circ}\text{C}$) [Saunders & Wahab, 1975].
 - Chain aggregation efficiency found to be temperature depended.
- Chains are observed in mid- to upper-level tropical, subtropical, and midlatitude summertime storms.
 - Cirrus anvils during CapeEx19 (Florida) where *in-situ* $E\text{-Fields} < 60 \text{ kV m}^{-1}$.
 - Deep stratiform cirrus anvils during ABFM-II (Florida) where *in-situ* $E\text{-Fields} < 60 \text{ kV m}^{-1}$.
 - Cirrus outflow during EMERALD-II (Darwin)
 - Convective cloud tops during CIRCLE-II (western Europe)
 - Overshooting tops during DC3 (eastern Colorado)



- The chain aggregation process is still not well understood.
 - Where and how do these aggregates form?
 - Laboratory results and aircraft observations are not in agreement.
- Chain aggregates are not represented in current cloud models.
- Recent observations of chain aggregates in cold-season storms (NASA IMPACTS) challenge existing theories and add uncertainty to our understanding.



Precipitation Formation

- Aggregation changes size/shape/fall speed → affects SIP, snowfall rates, and precipitation efficiency (Pasquier et al. 2023).

Radiative Impacts

- Elongated chains may have distinct optical properties vs. compact aggregates & single crystals → If so, can alter cloud radiative transfer and atmospheric energy balance (Baran, 2012; Um & McFarquhar, 2009).

Remote Sensing Interpretation

- The unique morphology of chains impacts radar and lidar retrievals, introducing biases in cloud microphysical retrievals (Westbrook et al. 2007).

Forecasting Uncertainties

- NWP microphysics schemes partition ice among a few assumed habits; if chains occur, fall-speed and scattering assumptions are incomplete, leading to systematic bias (Hashino, 2007; Karrer et al., 2021).

- **Document** in-situ evidence of chain aggregates in winter storms and clarify observational signatures. (*Paper 1*)
- **Build and validate** an automated classifier for chain vs. Non-chain aggregates in CPI imagery. (*Paper 2*)
- **Map and contextualize** chain aggregate occurrence across the IMPACTS campaign: along-track, 3-D placement with ER-2 context, storm lifecycle, and environment. (*Paper 3*)

1. **Paper 1 (*Chapter 2*): In situ Observations of Ice Crystal Chain Aggregates in Winter Storms**
 - a. In situ chain aggregates occur commonly in **weakly electrified winter storms**, not just in strongly electrified deep convection.
 - b. Chain aggregates appear across a **wide temperature/altitude range** and show **consistent plate/column morphology** (i.e., they're not confined to a narrow/specific cloud regime).
2. **Paper 2 (*Chapter 3*): Machine Learning Classification of Ice Crystal Chain Aggregates in Aircraft-Collected Cloud Particle Imagery**
 - a. A CNN trained on CPI imagery **can reliably distinguish chain aggregates** from other particle habits.
 - b. The CNN's performance and probability calibration hold on unseen flights/years, enabling threshold tuning to **minimize missed detections** without a disproportionate rise in false positives.
3. **Paper 3 (*Chapter 4*): Ice Crystal Chain Aggregates in Cold-Season Storms: Campaign-Scale Mapping and Contextualization**
 - a. **Chains peak in specific winter-storm regimes** and **storm-relative zones**, largely independent of strong electrification (lightning).
 - b. **High chain frequency aligns with coherent ER-2 radar/lidar signatures** usable for contextual prediction.



In situ Observations of Ice Crystal Chain Aggregates in Winter Storms

Paper 1 (Chapter 2)

- Unveiling observations of chain aggregates in winter storms (during IMPACTS).
 - ***First acknowledgment of chain aggregates within winter storms in literature***
- **Purpose:** Document in-situ winter occurrences of ice crystal chain aggregates and establish a clear working definition.
- **Scope:** Survey across the IMPACTS campaign (multi-year, multi-storm), using CPI and PHIPS imagery for cross-validation.
- Provides a standardized identification protocol and a curated set of time/altitude/temperature contexts for chain occurrences.
- We don't quantify mechanisms or storm-wide frequencies; this paper is an observational baseline.
- Creates the labeled foundation for **automated detection (Paper 2)** and **campaign-scale mapping/context (Paper 3)**.

- Data: CPI IMAGES FROM ALL IMPACTS FLIGHTS
- **Targeted review:** Image sequences selected using the cloud-probe operator's flight notes indicating approximate times of aggregate sightings.
- **CPI collages (1-min):** For each flagged period, generated 1-minute CPI collages (4×3 grid of particle images over 5-s intervals).
- **Manual identification protocol:** Reviewed all 1-min collages; any 5-s interval with ≥ 3 identifiable chains was marked as a chain occurrence.
- **Recorded context:** For each occurrence, logged flight date, 5-s interval, temperature, and altitude range.

- Chain aggregates are identified on 28 of 34 IMPACTS flights
 - Cover approximately 1,242 minutes of the 12,943 minutes of total P-3 flight time (~10%; Table 1)
 - 3,360 minutes in 2020
 - 4,166 minutes in 2022
 - 5,417 minutes in 2023
- Flight times include in-cloud sampling, transits between sampling segments (legs), and ferry time.

Likely an Upper-bound

Table 1. Summary of chain aggregate observations during the 2020, 2022, and 2023 IMPACTS field deployments. Columns indicate the number of flights in which chain aggregates were observed, total observation time when chains were observed (minutes), the respective temperature range and average temperature, altitude range and average altitude, and the number of colocated P-3 and ER-2 flight legs where chain aggregates were present.

| Year | Flights (#) w/ Chains | Approx. # of Minutes | $T_{min} - T_{max}, \bar{T}$ [°C] | $Z_{min} - Z_{max}, \bar{Z}$ [km] | # of Collocated Legs (Chains) |
|------|-----------------------|----------------------|-----------------------------------|-----------------------------------|-------------------------------|
| 2023 | 11 | 386.8 | -30.8 to -1.2, -17.7 | 2.0 - 9.7, 5.5 | 10 |
| 2022 | 9 | 425.8 | -38.2 to 0.8, -22.7 | 1.5 - 9.0, 5.8 | 6 |
| 2020 | 8 | 429.0 | -32.2 to 2.5, -10.6 | 1.5 - 7.7, 4.5 | 5 |

Paper 1 – Results

- Observed across the full range of temperatures and altitudes (Fig. 4).
- Composed of a variety of individual crystal habits (primarily columnar and plate-like).
 - Consistent with previous field studies (Connolly et al. 2005; Nairy, 2022).
- Predominantly $D_{max} > 500 \mu\text{m}$
 - Similar to cirrus anvil observations (Nairy et al. 2022).
- Composed of pristine ice crystals, others show signs of sublimation
 - Similar to cirrus anvil observations (Nairy et al. 2022).

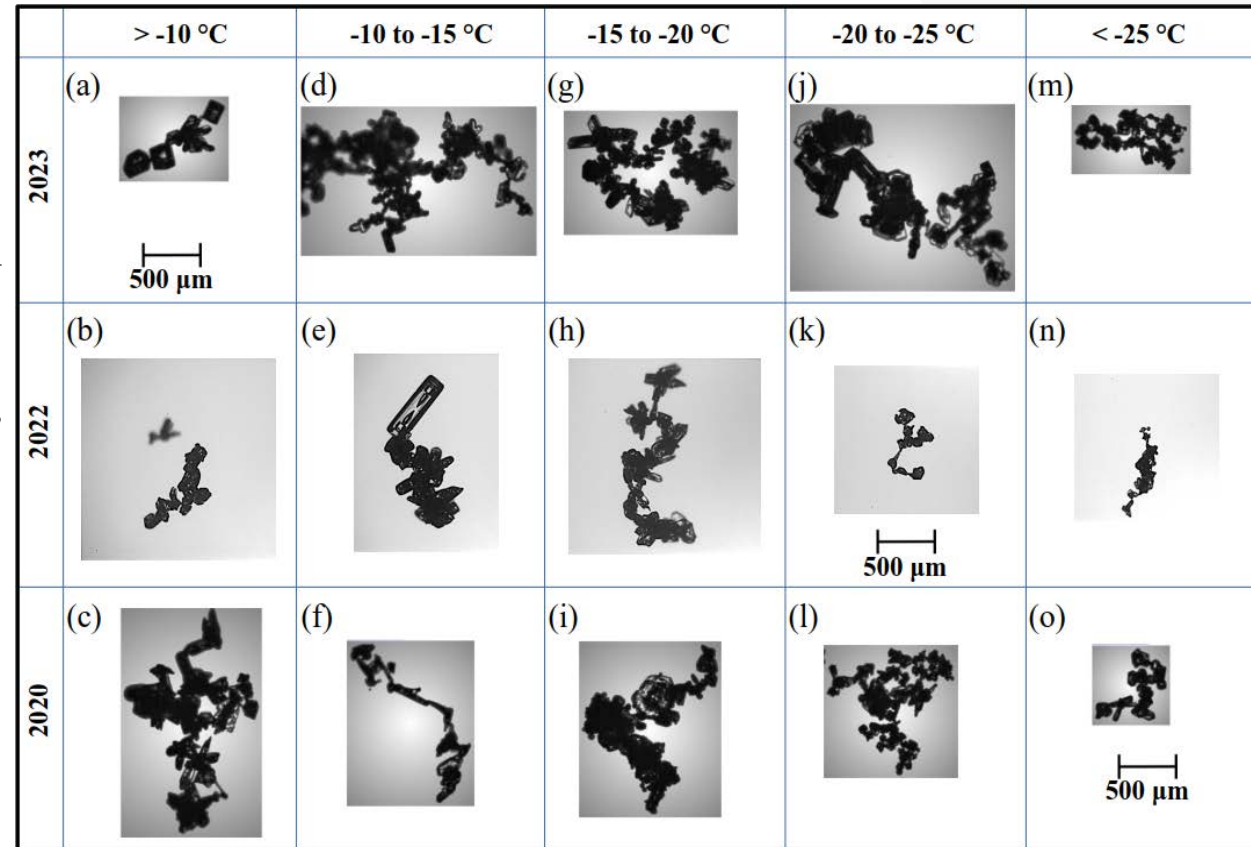


Figure 4. Illustration showing representative chain aggregate images observed during the NASA IMPACTS field campaign grouped by deployment year and temperature intervals. The image labels give the UTC date and time. The 2023 and 2020 rows contain Hawkeye Cloud Particle Imager (CPI) images, while the 2022 row contains PHIPS probe images.

Paper 1 – Discussion

Example of using colocated dataset.

19 Jan 2022 Flight Segment

- 12:30 – 12:55 UTC
- ~ 6 km AGL
- 9,315 CPI Images Classified

Chain Aggregates Observed:

- -31.5 to -29.5 °C
- Relatively weak dBZ_e (-16.07 ± 5.53 dBZ_e)
- Minimal V (-0.38 ± 0.91 m s⁻¹)
- Moderate CPL β_{532} (-2.38 ± 0.37 km⁻¹ sr⁻¹)
- Modest CPL δ and CRS LDR (0.34 ± 0.06 and -17.38 ± 2.34 dB, respectively)

- No LIP electric field data for this pass.

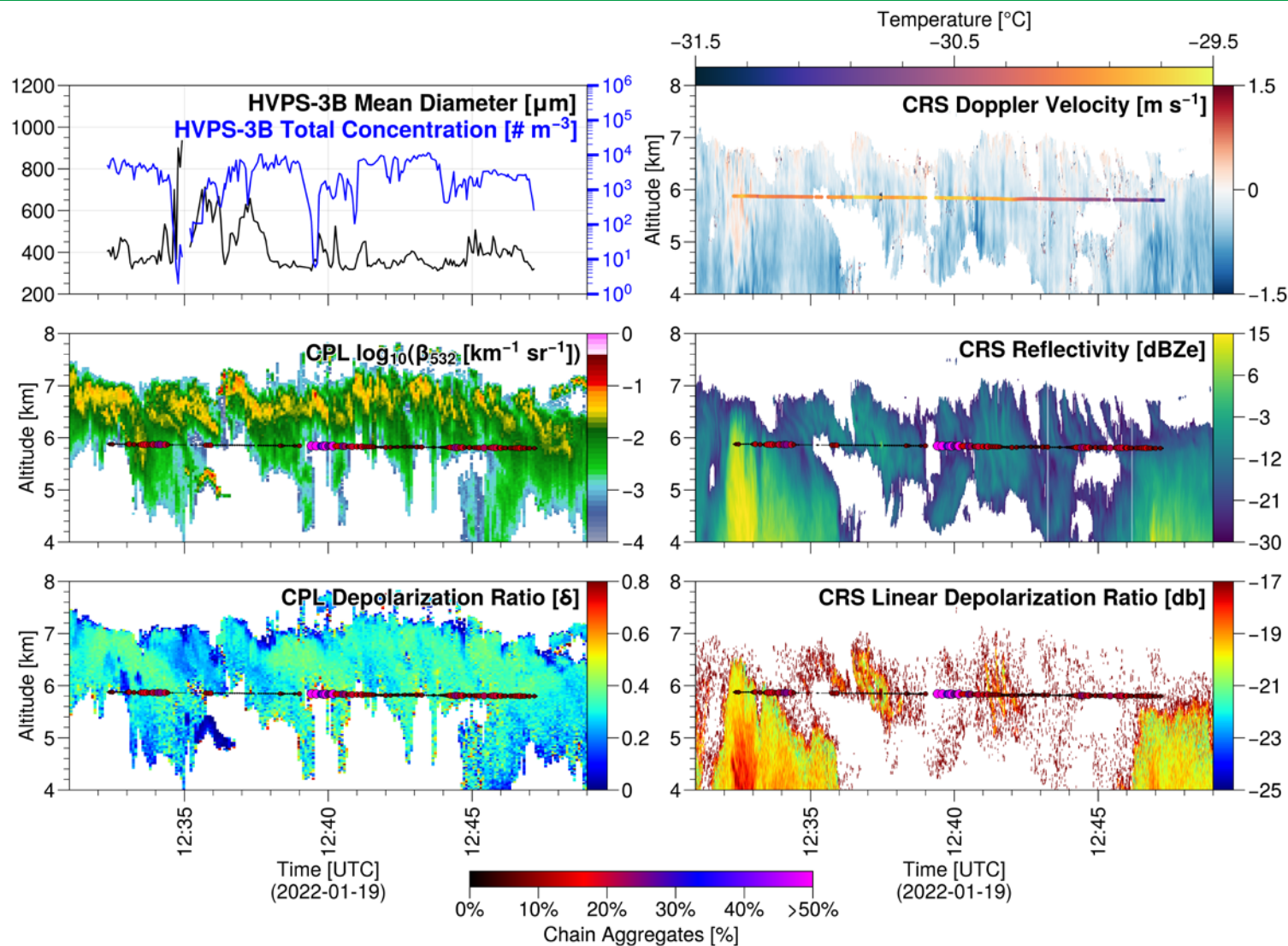


Figure 5. Plots showing colocated in-situ and remote sensing observations obtained by the NASA P-3 and ER-2 aircrafts on 19 January 2022.

Paper 1 – Discussion

- This single-case analysis shows no simple correlation between chain aggregate occurrence and the available remote-sensing parameters on the ER-2.
- Underscores the need to analyze additional IMPACTS cases (ideally stratified by environment/altitude) to assess whether relationships emerge under different conditions or scales.

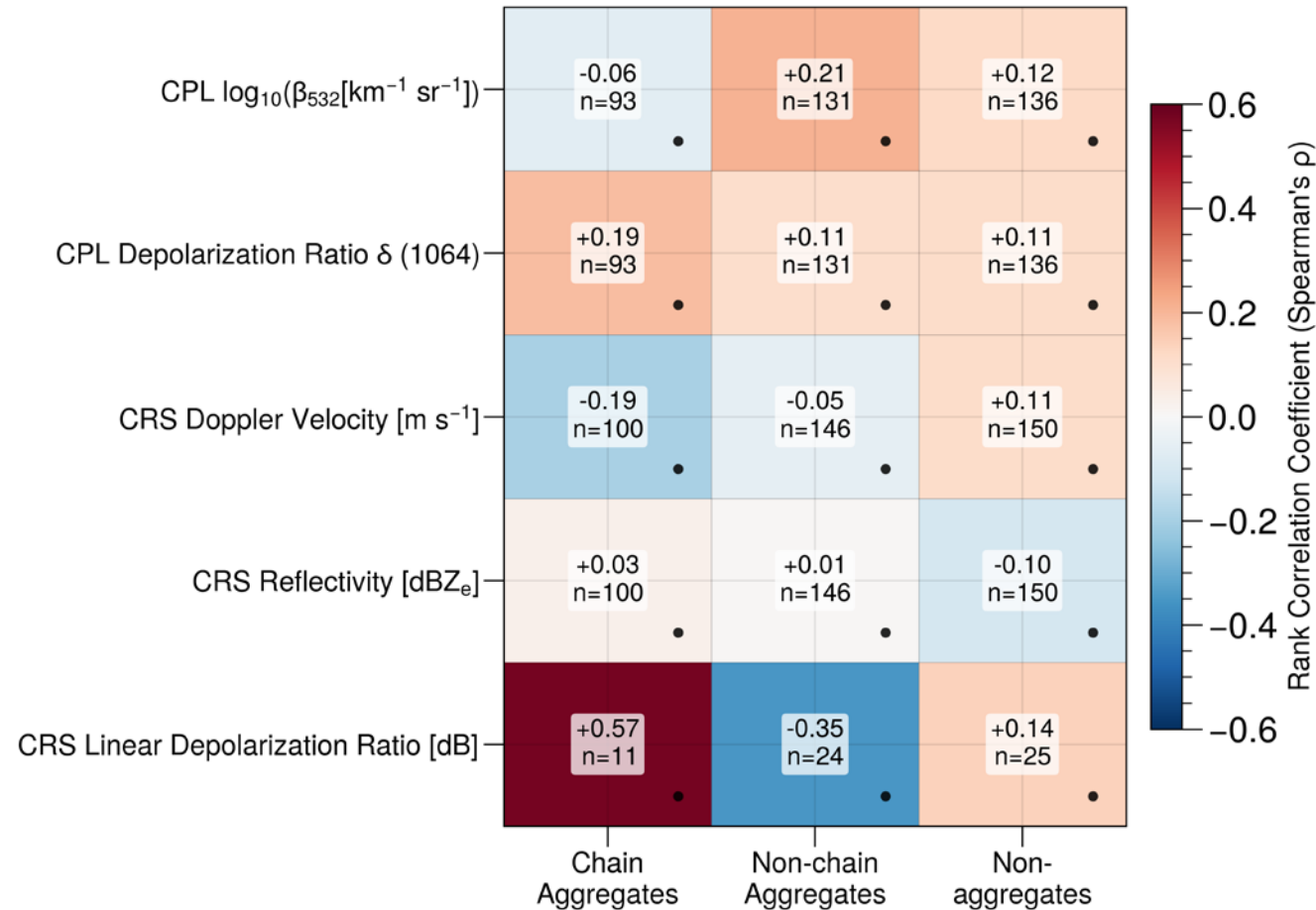


Figure 6. Rank correlation coefficients (Spearman's ρ) between 5-second particle counts and collocated remote-sensing metrics for the 2022-01-19 ER-2/P-3 matched segment. Rows show: CPL β_{532} , CPL depolarization ratio (δ , 1064 nm), CRS Doppler velocity [m s^{-1}], CRS equivalent reflectivity [dBZ_e], and CRS linear depolarization ratio [dB]. Columns separate Chain Aggregates, Non-chain Aggregates, and Non-aggregates. Each cell lists linear correlation (Spearman ρ) and the number of 5-second bins (n); only bins with ≥ 1 particle in that class are included. Bullets indicate values that are not statistically significant after Benjamini-Hochberg false-discovery-rate correction ($q = 0.05$).

- 23 July 2025 - Submitted to American Geophysical Union (AGU) - Geophysical Research Letters (GRL)
- Accepted pending minor revisions (04 November 2025)
- Revisions submitted 17 November 2025

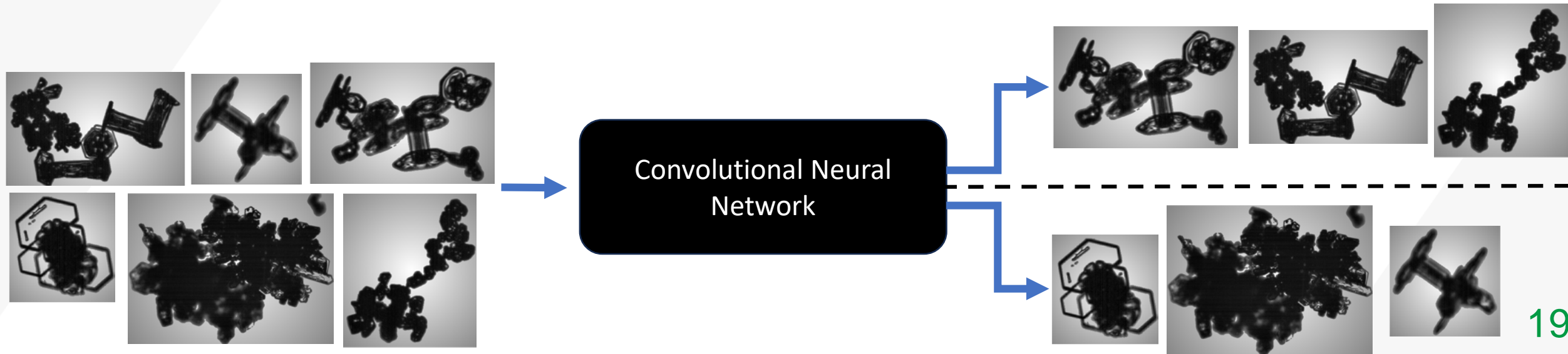


Machine Learning Classification of Ice Crystal Chain Aggregates in Aircraft-Collected Cloud Particle Imagery

Paper 2 (Chapter 3)

Understanding chain aggregate formation within cloud systems requires contextual analysis, but manual classification of cloud particles is extremely time-consuming.

Objective: Employ a supervised Convolutional Neural Network (CNN) to differentiate ice crystal chain aggregates from non-chain aggregates.



Paper 2 – Data & Methods

1. Utilize 56,193 manually classified ice crystals ($D_{\max} > 150 \mu\text{m}$) obtained from Cloud Particle Imager (CPI) observations during NASA's IMPACTS field campaign.
2. Train, validate, and evaluate multiple CNN architectures.
3. Identify the most effective CNN for distinguishing chain aggregates.
4. Apply the best CNN model to classify CPI data from other IMPACTS flights.

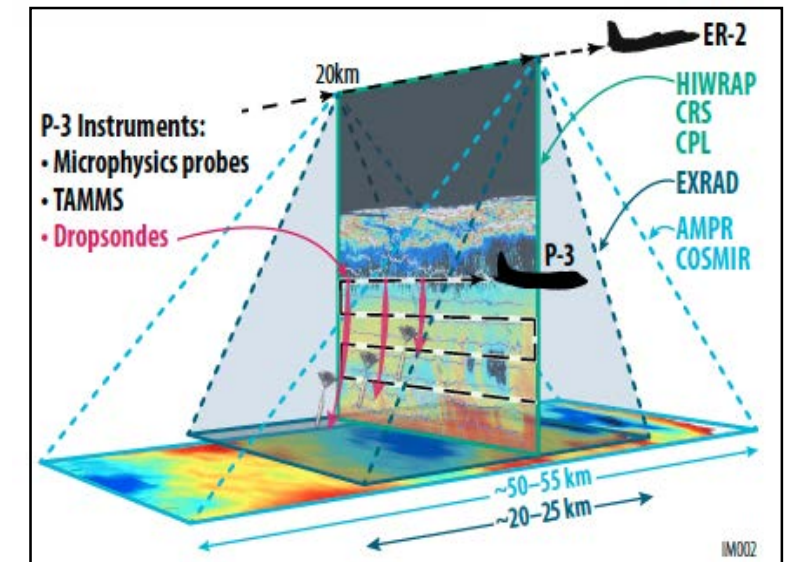
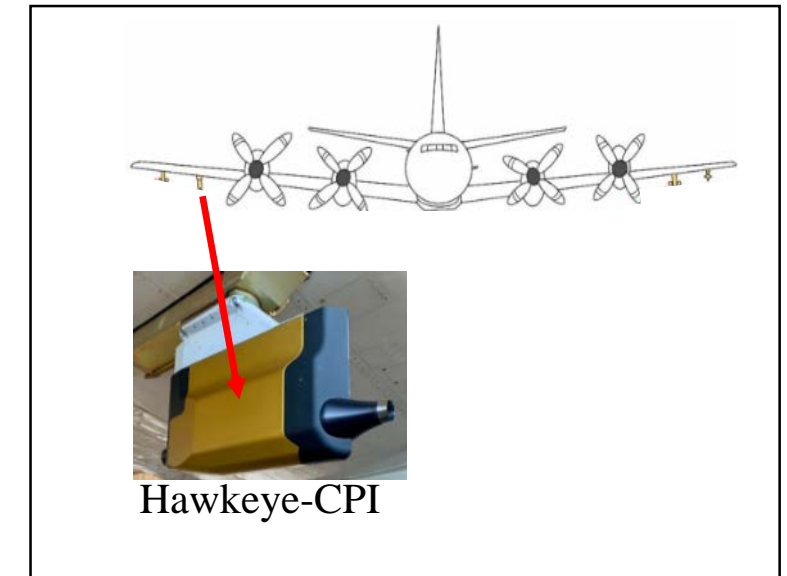
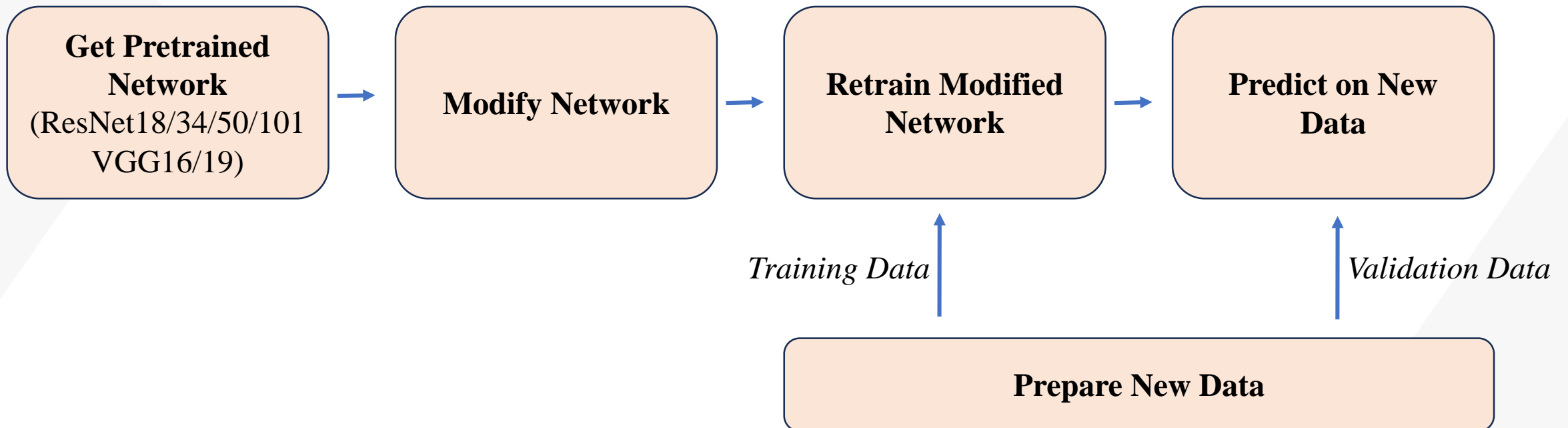


Figure 7. Plots showing collocated in-situ and remote sensing observations obtained by the NASA P-3 and ER-2 aircrafts on 19 January 2022.

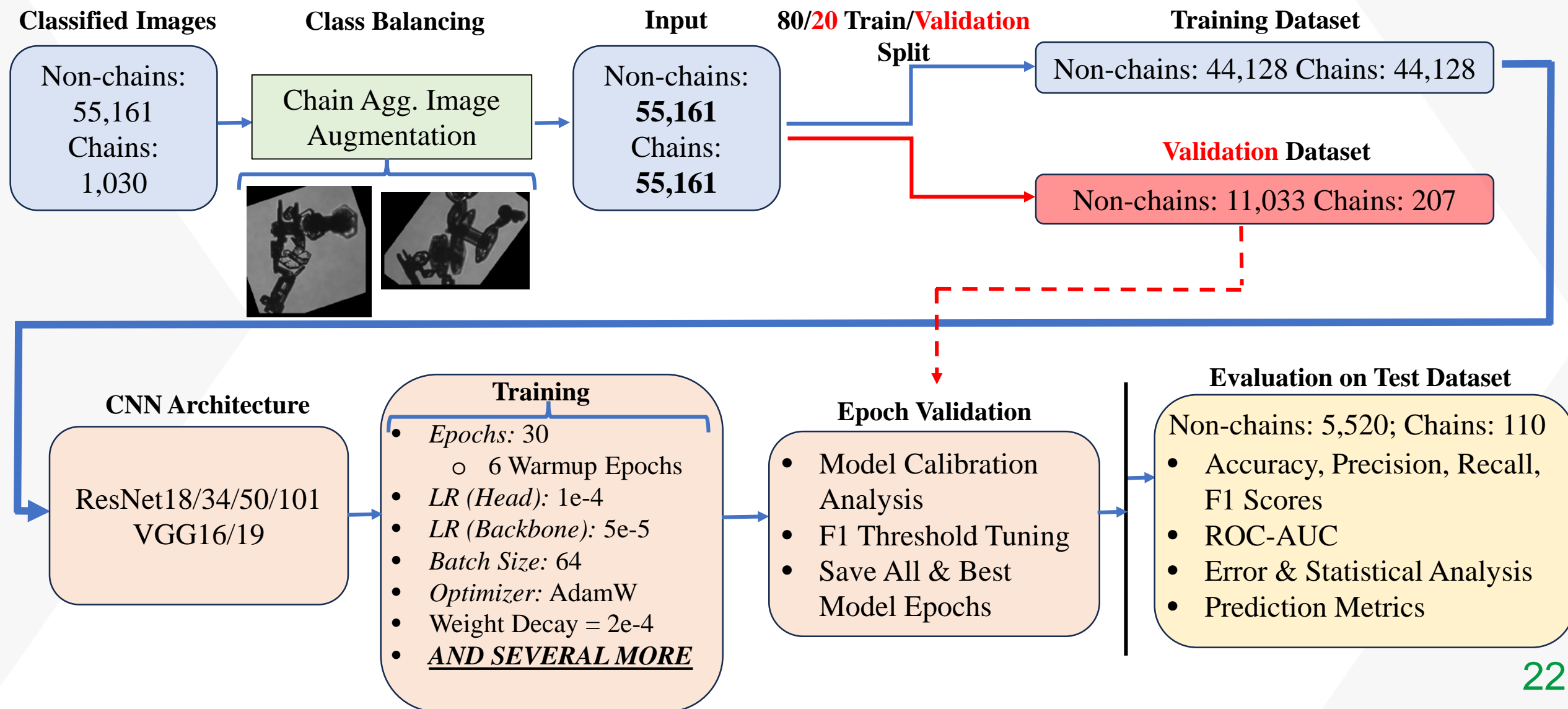
Transfer Learning in Convolutional Neural Networks for Image Classification

- **What it is:** Reusing a model trained on a large, related dataset and fine-tuning it for your new task instead of starting from scratch.
- **Why it helps:** You inherit useful features and good initial weights, so you typically need less data, converge faster, and get better accuracy.



Paper 2 – Data & Methods

End-to-End CNN Pipeline for Chain Aggregate Classification



How will we know if a CNN is "good" enough?

1. **Primary:** High precision on the chain aggregate class in external validation.
2. **Secondary:** Strong precision rate-area under curve (PR-AUC) and ROC-AUC across folds.
3. **Reliability:** Low log-loss and low Brier score, plus good calibration.

Model choice is based on **precision first**, then stability (spread across folds), then threshold-free metrics (F1-score; recall).

Paper 2 – Results

- **ResNet34** leads on PR-AUC and shows the lowest LogLoss and Brier, with tight variability → best calibrated and most reliable.
- ResNet50/ResNet101 post strong ROC-AUC and competitive PR-AUC, with moderate calibration (LogLoss/Brier) and small spread.
- Lagging models: VGG16 (and to a lesser extent VGG19) show higher LogLoss/Brier and lower PR-AUC with wider spread → weaker calibration and precision–recall performance.

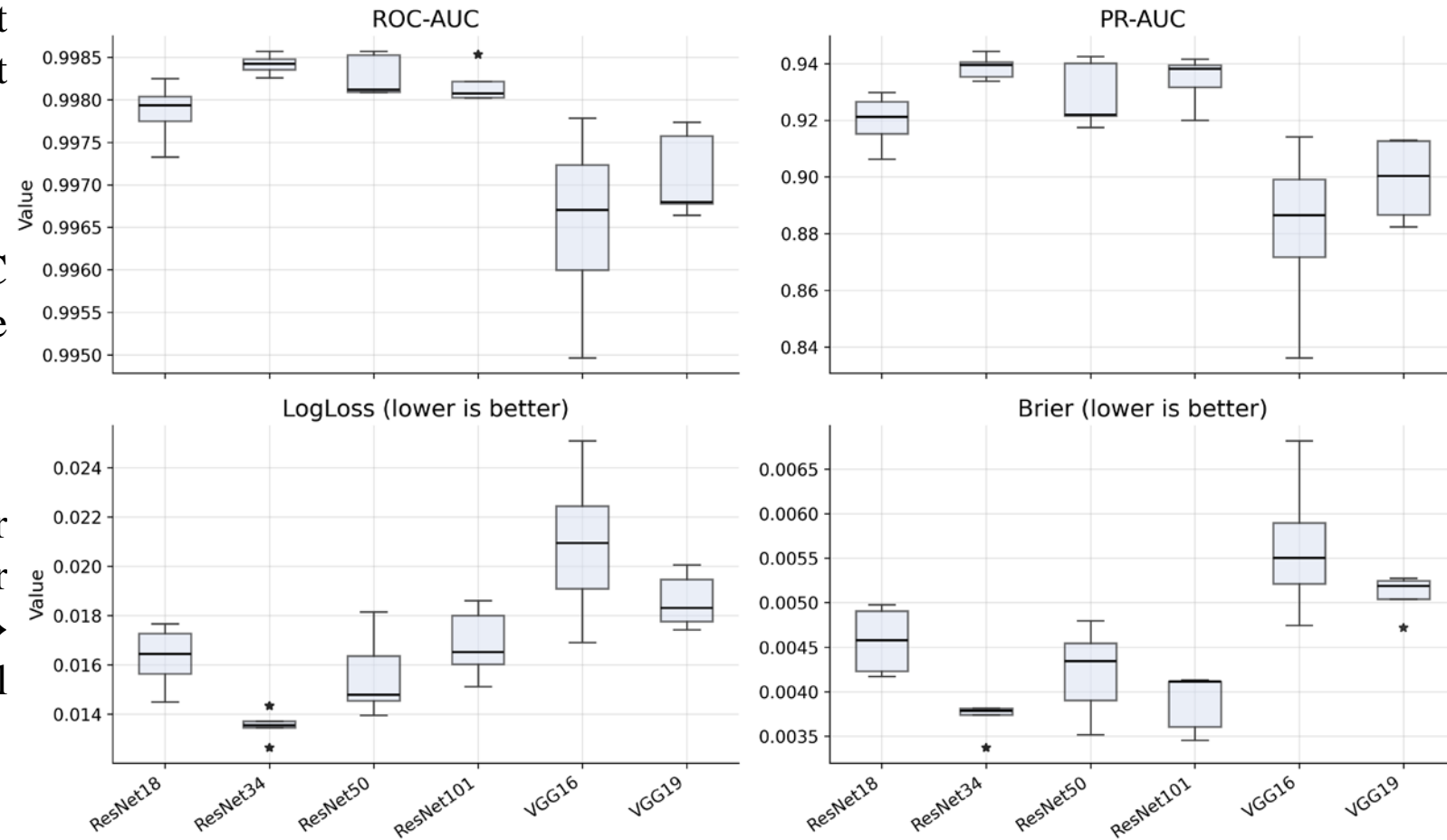


Figure 5. Validation boxplots comparing six CNNs across folds for (top-left) ROC-AUC, (top-right) PR-AUC, (bottom-left) LogLoss (lower is better), and (bottom-right) Brier score (lower is better). Boxes show IQR with median lines; whiskers denote non-outlier ranges.

Paper 2 – Results

Priority: Precision

- ResNet34: highest mean/median precision (~0.92–0.93) with tight spread.
- VGG19: high precision but wider variability; center is a bit lower than ResNet34.
- ResNet101: slightly below ResNet34 in precision (~0.90–0.92).

Best Balance

- ResNet101 gives the best precision–recall tradeoff and tightest spread → more reliable across folds.

Middle Tier.

- ResNet/18/50: solid precision (~0.85–0.91), mid recall, moderate spread.

Lower Performer.

- VGG16: lower precision and the widest spread → least dependable for minimizing false positives.

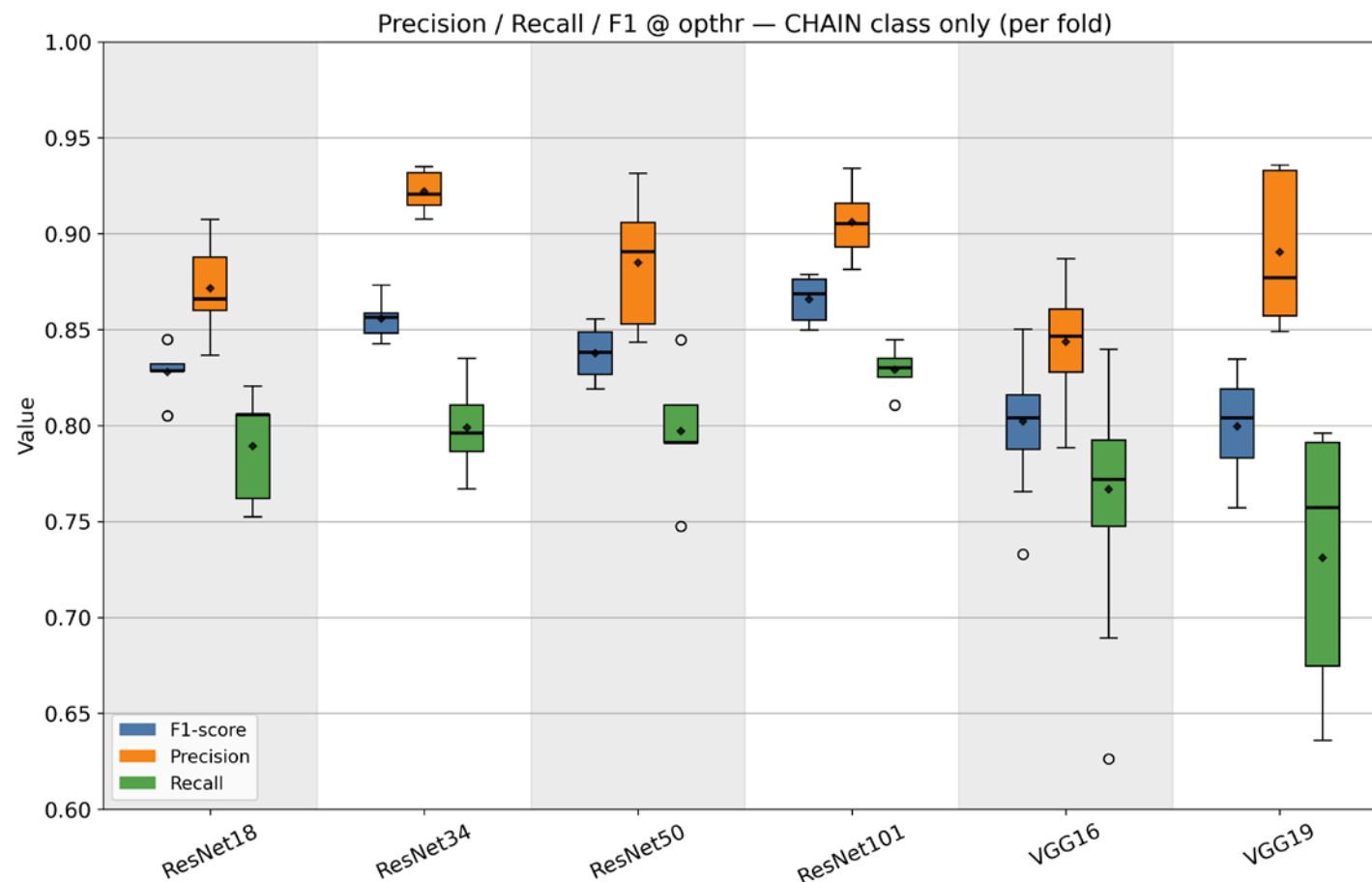


Figure 8. Boxplots of precision, recall, and F1 for the CHAIN class at the operating threshold (opthr) from external validation across folds for each CNN (ResNet18/34/50/101, VGG16/19). Boxes show the interquartile range with medians, whiskers extend to 1.5×IQR, and outliers are plotted as points; light bands alternate by model.

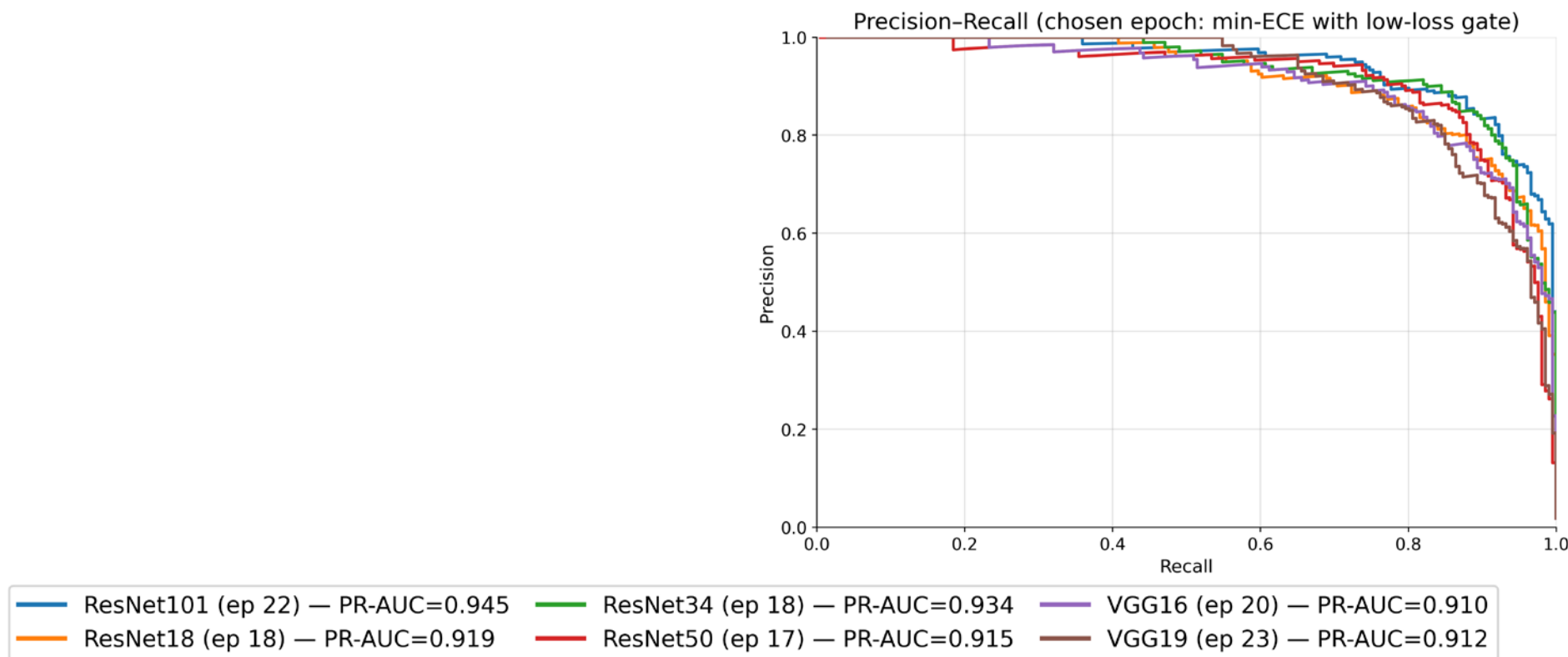


Figure 9. Model comparison at the chosen epoch (minimum ECE within 10% of each model's lowest validation loss). Left: Calibration curves (binwise predicted probability vs. observed positive fraction); proximity to the 1:1 dashed line indicates better calibration. Right: Precision-Recall curves for the same epochs

- ResNet101 (and closely ResNet34) delivers the strongest discrimination (highest PR-AUC) while staying closest to the 1:1 calibration line at the chosen low-loss.
- ResNet101 and ResNet34 keep precision >0.85 up to ~ 0.85 – 0.9 recall, while VGG16/19 lose precision earlier (~ 0.8 recall falls to ~ 0.7 – 0.8). ResNet50 is mid-pack.

Paper 2 – Results

- Emphasizes high precision on the CHAIN class (few false positives).
- Missed detections are limited relative to total positives (balanced with your “minimize missed detections” priority).
- Numbers align with PR curve shape (strong precision into high recall).

At the chosen threshold (> 0.671), ResNet34 delivers **few false alarms** while retaining **strong CHAIN** detection.

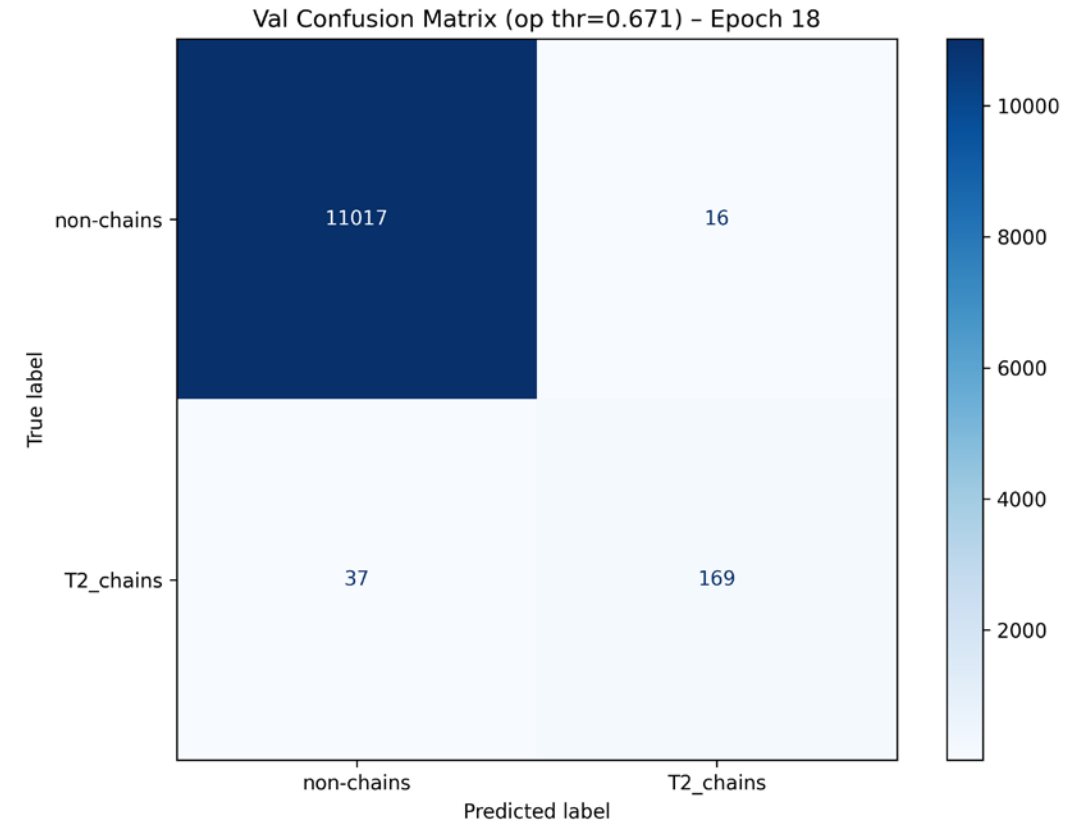
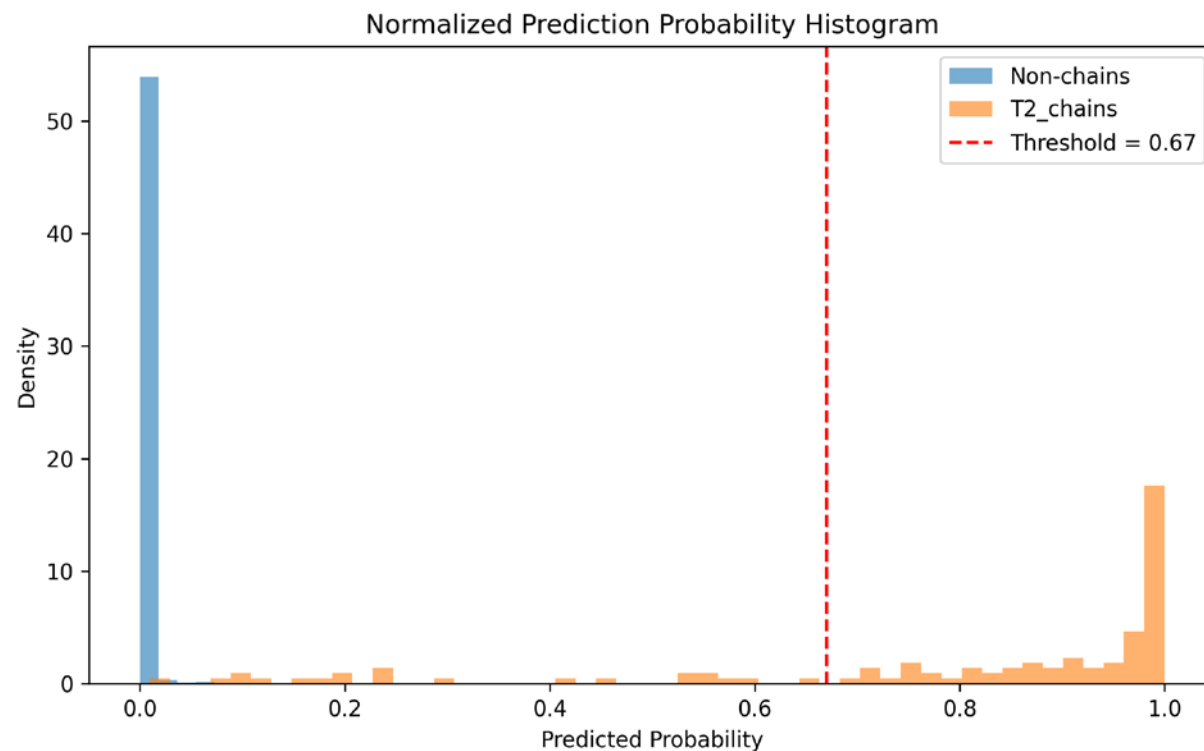
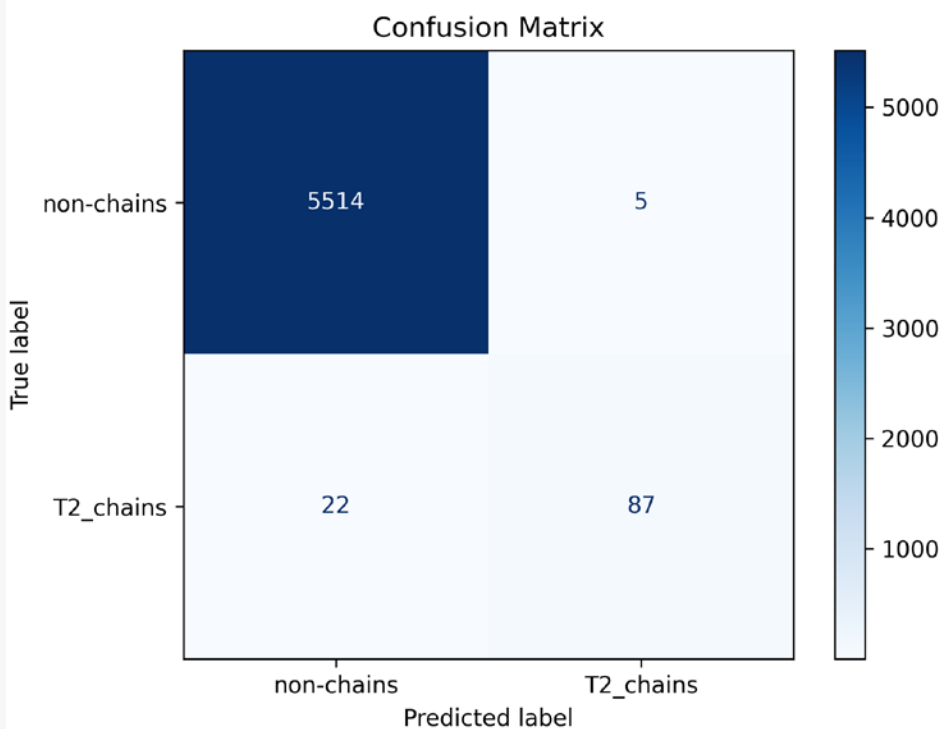


Figure 10. Confusion matrix of the best performing epoch of ResNet34 using an operational threshold (op thr) > 0.671 .

Results on Test (Unseen) Data: (*Non-chains: 5,519; Chains: 109*)





| | Precision | Recall | F1-Score | Support |
|---------------------|-----------|--------|----------|---------|
| Non-chains | 100 % | 100% | 100% | 5519 |
| Chain Aggregates | 95% | 80% | 87% | 109 |
| Macro Avg. Accuracy | 97% | 90% | 93% | 5628 |

- **Calibration & reliability:** ResNet34 has the lowest LogLoss/Brier and tight spread → most reliable across folds.
- **Discrimination:** ResNet101 edges highest PR-AUC in several runs; ResNet34 is a close second but steadier.
- **Operational implication:** For minimizing false positives, both ResNet34 and ResNet101 are suitable; ResNet34's stability + calibration makes it the safer default.

Why ResNet > VGG?

- Residual connections make deeper models easier to train, preserve important fine-scale CPI features, and reduce overfitting, giving better generalization on our limited, highly specialized dataset.

Why ResNet34?

- ResNet18  Over Generalization
- > ResNet34  Too Complex (Deep)

- A CNN can reliably separate chain aggregates vs. non-chain CPI images using transfer learning.
- **ResNet34** shows best overall reliability (LogLoss/Brier) with competitive PR-AUC.
- Calibration-aware selection (min-ECE under a low-loss gate) yields well-tuned epochs for robust external validation.
- Results from testing the trained ResNet34 model on unseen data verifies that we can be confident in its output.

1. Validated, calibration-aware CNN pipeline for chain aggregate detection in aircraft CPI imagery.
2. The CNNs are readily available and can be reused by anyone interested in identifying chain aggregate occurrences from CPI images.
3. Work is being done to allow the CNN to be active for real-time in situ sampling.

This work establishes a dependable, well-calibrated classifier that unlocks campaign-scale chain aggregate analysis.

Manuscript Status:

- Introduction, Methods, and Data sections are written.
- Skeleton of the results, discussion, and conclusion sections
- All figures for results and discussion sections have been generated.

Estimate date of first draft completed: **February 2026**

Plan to submit manuscript to Journal of Atmospheric and Oceanic Technology (JTECH). **Estimate submission date is March 2026.**



Ice Crystal Chain Aggregates in Cold-Season Storms: Campaign-Scale Mapping and Contextualization

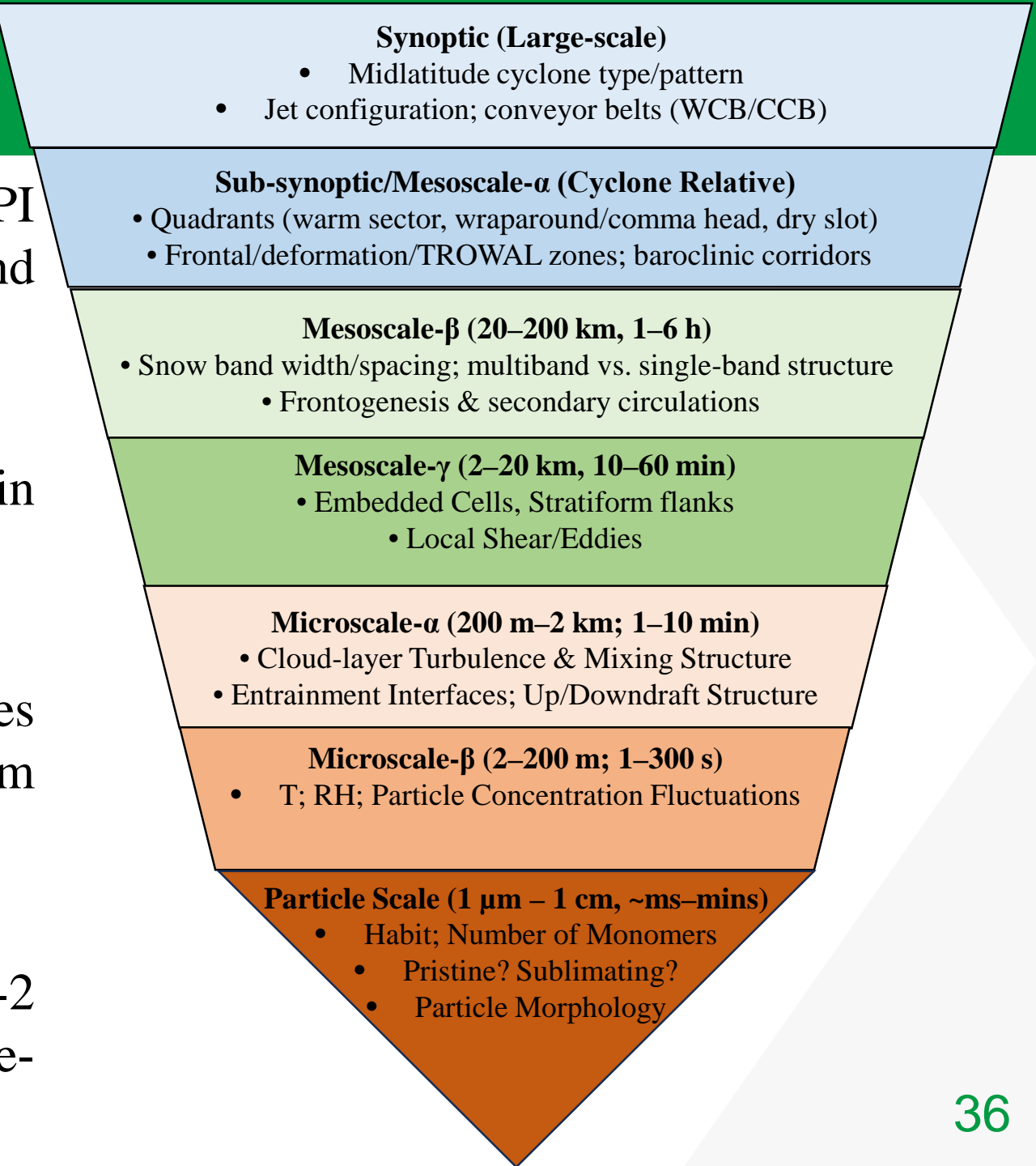
Paper 3 (Chapter 4)

1. Use the calibrated CNN from Paper 2 to classify all IMPACTS CPI images as “chain” or “non-chain” and build a campaign-wide database of chain aggregate occurrences.
2. Merge CNN-identified chains with P-3 in situ measurements, ER-2 radar and lidar, and ancillary fields to place each occurrence in its storm-relative and environmental context.
3. Map and analyze chain aggregate frequency and characteristics across meteorological scales from synoptic to particle scale to determine where, when, and under what conditions chains are most common.

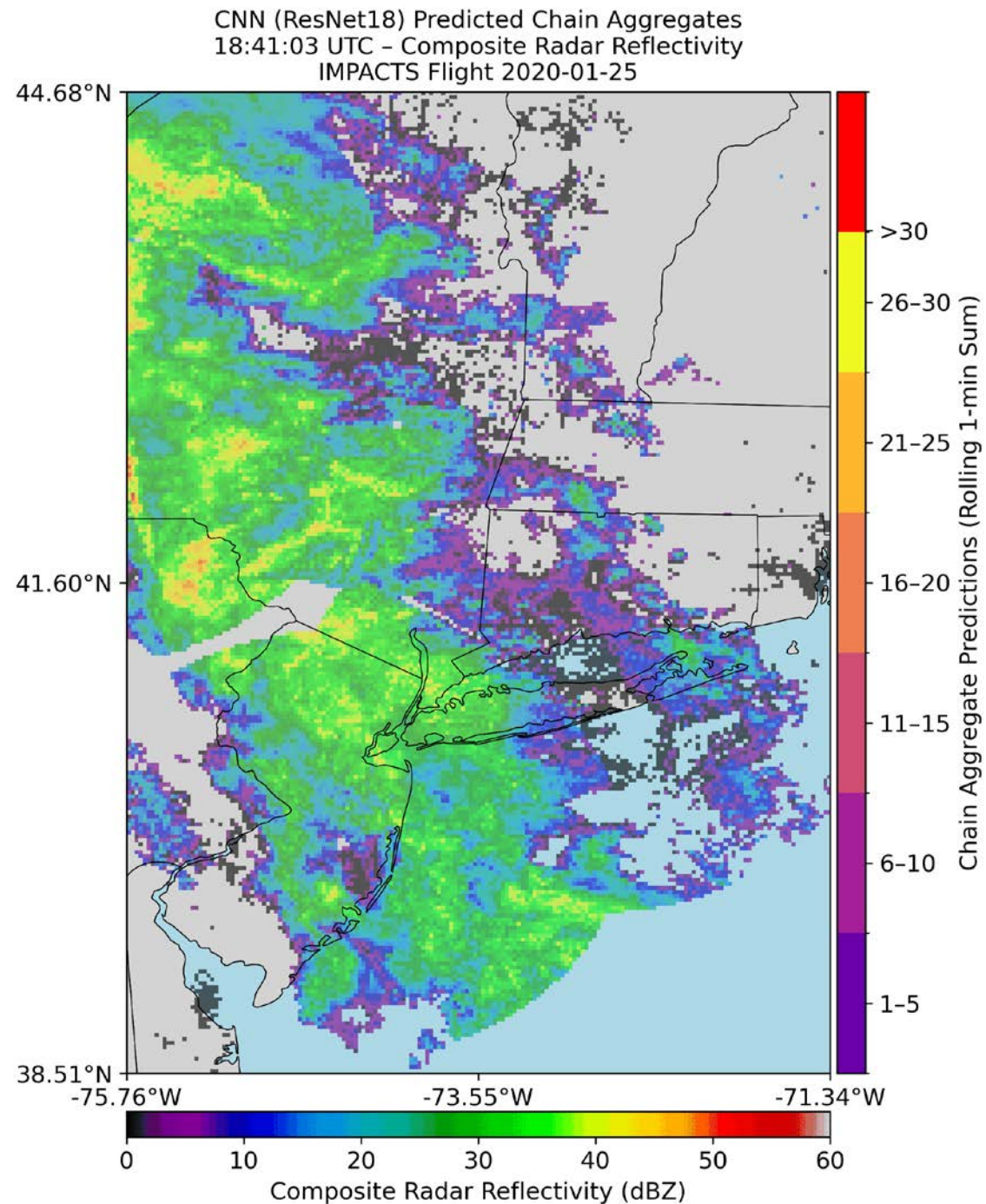
- **IMPACTS dataset:** 33 Intensive Operating Periods (IOPs); 34 including flight to WP-AFB
- **CNN inputs:** All CPI particle images from 2020, 2022, and 2023, including periods with and without chain aggregates.
- **Collocated ER-2 remote sensing:** CRS radar reflectivity, Doppler velocity, and linear depolarization ratio; CPL backscatter and depolarization ratio.
- **Environmental fields:** Thermodynamic and kinematic fields from reanalysis (temperature, RH, vertical motion, frontogenesis, shear).
- **Storm-scale context:** Radar mosaics and satellite imagery (e.g., NEXRAD composites, GOES) to identify cyclone structure, snow bands, and storm phase for each case.

Paper 3 – Methods

- Run the CNN (Paper 2) on all IMPACTS CPI images to get chain/non-chain labels and probabilities.
- Analyze chain occurrence and properties within a nested meteorological scale framework.
- Map detections into storm-relative coordinates (cyclone center, fronts, conveyor belts; warm sector, wrap-around, dry slot).
- Bin detections in space and time for P3/ER-2 collocation analysis (Mesoscale- γ to Microscale- β).



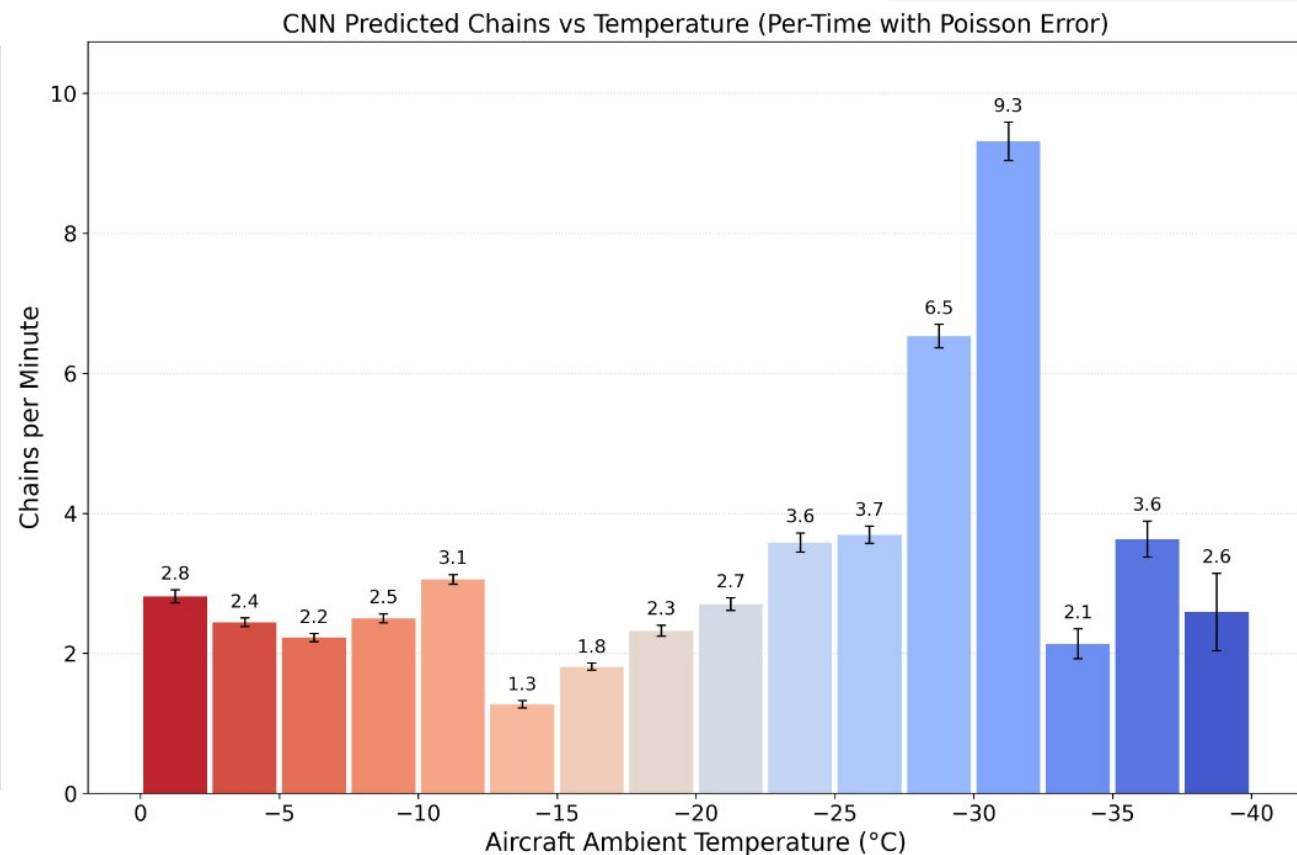
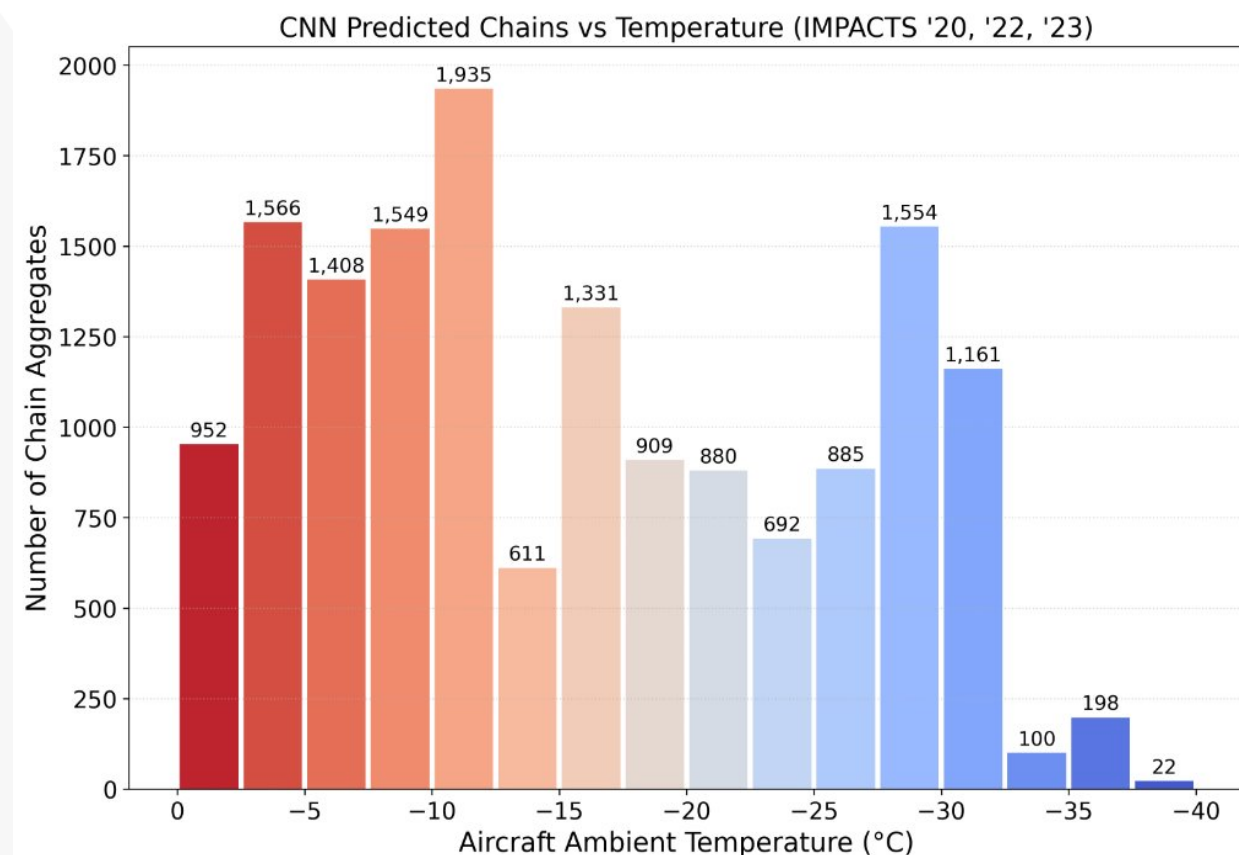
Paper 3 – Preliminary Results



CNN (ResNet18) Predicted Chain Aggregates
20:41:03 UTC - Composite Radar Reflectivity
IMPACTS Flight 2020-01-25



Paper 3 – Preliminary Results



- CNN normalized chain aggregate rates w.r.t. temperature show peaks at $\sim 30^{\circ}\text{C}$.

- Demonstrate a transferable workflow that combines CNN classification with in-situ and remote sensing data for cloud microphysics studies.
- Link chain aggregate occurrence to storm-relative structure.
- Advance understanding of (chain) aggregation processes to support better ice microphysics parameterizations in models.

- **Document** in situ evidence of chain aggregates in winter storms and clarify observational signatures. (*Paper 1*)
 - Foundational paper motivating further analysis.
- **Build and validate** an automated classifier for chain vs. Non-chain aggregates in CPI imagery. (*Paper 2*)
 - Tools Paper
- **Map and contextualize** chain aggregate occurrence across the IMPACTS campaign: along-track, 3-D placement with ER-2 context, storm lifecycle, and environment. (*Paper 3*)
 - Meteorological Paper

Collaborations – Non-dissertation Research

2022

1. Delene et al. (2022). **Particle Shattering Analysis of Airborne Microphysical Probes Using IMPACTS Observations**
2. Majdi et al. (2022). **An Evaluation of a Convolutional Neural Network for Classifying Images from In-situ Cloud Probes**

2023

1. Finlon et al (2023). **Relating Lidar Measurements to Cloud Microphysical Properties During IMPACTS**

2024

1. Finlon et al. (2024). **Disentangling Cloud Microphysical Properties from Lidar Backscatter and Depolarization Measurements in Winter Storms During the IMPACTS Field Campaign**
2. McFarquhar et al. (2024). **Use of In-Situ Airborne Measurements of Cloud Microphysical Properties to Quantify Processes Occurring in Wintertime Snow Storms**
3. Dunnavan et al. (2024). **Improving Understanding of Ice Particle Shapes and Orientations: Reconciling 2D-S Cloud Probe Observations with Theoretical Simulations – *In Prep***
4. Co-authored NASA MOSAICS proposal. **Unveiling Ice Crystal Chain Aggregates in Winter Storms: Contextualization using In-situ and Remote-sensing Observations – *Funded, Dollar Value - \$399,995; Project Duration 05/16/2025 - 05/15/2027***

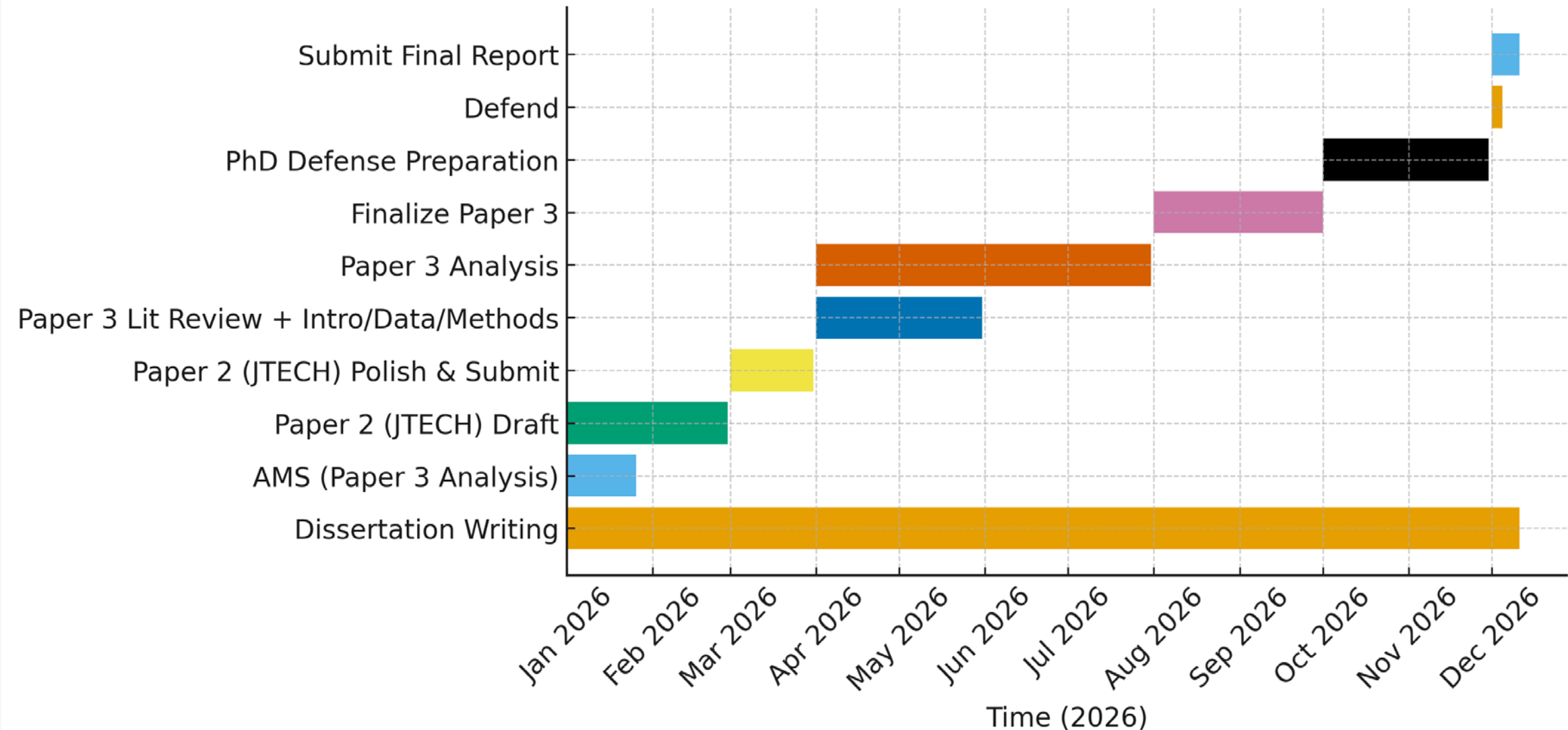
2025

1. Osmani et al. (2025). **Investigating Atmospheric Ice Crystal Formation and Their Impacts on Hypersonic Vehicles – *Published***
2. Finlon et al. (2025). **Influence of Cloud Microphysical Properties on Airborne Lidar Measurements: Results from the IMPACTS Field Campaign – *Published***
3. Delene et al. (2025). **Cloud Microphysical Observations of Seeded Clouds during the Saudi Arabia AeRosol-Cloud-Precipitation Enhancement Campaign (SARPEC) - *In Review***
4. Ojo et al. (2025). **A Low Temperature Dual Balance Electrodynamic Trap (LT-DBET) for Atmospheric Ice Crystal Aggregation**
5. Delene et al. (2025). **Quantification of Chain Aggregate Morphology in Recent Field Campaigns**

For complete listing see:
[Full List of Collaborations](#)

Timeline to Graduation

PhD Timeline Gantt Chart (2026)



- Baran, A. J. (2012). From the single-scattering properties of ice crystals to climate prediction: A way forward. *Atmospheric Research*, 112, 45–69. <https://doi.org/10.1016/j.atmosres.2012.04.010>
- Connolly, P. J., Saunders, C. P. R., Gallagher, M. W., Bower, K. N., Flynn, M. J., Choularton, T. W., et al. (2005), Aircraft observations of the influence of electric fields on the aggregation of ice crystals. *Quarterly Journal of the Royal Meteorological Society*, 131(608), 1695–1712. <https://doi.org/10.1256/qj.03.217>.
- Dye, J. E., Bansemer A. (2019), Electrification in Mesoscale Updrafts of Deep Stratiform and Anvil Clouds in Florida. *Journal of Geophysical Research: Atmospheres*, 124(2), 1021–1049, <https://doi.org/10.1029/2018JD029130>
- Dye, J. E., Bateman, M. G., Christian, H. J., Defer, E., Grainger, C. A., Hall, W. D., et al. (2007), Electric fields, cloud microphysics, and reflectivity in anvils of Florida thunderstorms. *Journal of Geophysical Research: Atmospheres*, 112(D11). <https://doi.org/10.1029/2006JD007550>
- Finnegan, W. G., & Pitter, R. L. (1988), A postulate of electric multipoles in growing ice crystals: Their role in the formation of ice crystal aggregates. *Atmospheric Research*, 22(3), 235–250. [https://doi.org/10.1016/0169-8095\(88\)90019-1](https://doi.org/10.1016/0169-8095(88)90019-1)
- Gayet, J.-F., Mioche, G., Bugliaro, L., Protat, A., Minikin, A., Wirth, M., et al. (2012), On the observation of unusual high concentration of small chain-like aggregate ice crystals and large ice water contents near the top of a deep convective cloud during the CIRCLE-2 experiment. *Atmospheric Chemistry and Physics*, 12(2), 727–744. <https://doi.org/10.5194/acp-12-727-2012>
- Nairy, C. M. (2022), Observations of Chain Aggregates in Florida Cirrus Cloud Anvils on 3 August 2019 during CAPEEX19 (Master's thesis), Dept. of Atmospheric Sciences, University of North Dakota, Grand Forks, North Dakota. Retrieved from <https://commons.und.edu/theses/4363/>
- NCAR/EOL. (2020). IMPACTS 2020 Field Catalog. https://catalog.eol.ucar.edu/impacts_2020/
- NCAR/EOL. (2022). IMPACTS 2022 Field Catalog. https://catalog.eol.ucar.edu/impacts_2022/
- NCAR/EOL. (2023). IMPACTS 2023 Field Catalog. https://catalog.eol.ucar.edu/impacts_2023/
- Pasquier, J. T., Henneberger, J., Korolev, A., Ramelli, F., Wieder, J., Lauber, A., et al. (2023). Understanding the History of Two Complex Ice Crystal Habits Deduced From a Holographic Imager. *Geophysical Research Letters*, 50(1). <https://doi.org/10.1029/2022GL100247>
- Um, J., & McFarquhar, G. M. (2009). Single-scattering properties of aggregates of plates. *Quarterly Journal of the Royal Meteorological Society*, 135(639), 291–304. <https://doi.org/10.1002/qj.378>